JOURNAL OF SOLID STATE CHEMISTRY 5, 300–313 (1972)

Vacancy and Charge Ordering in the Th_3P_4 Related Structures

FORREST L. CARTER

Naval Research Laboratory, Washington, D.C. 20390

Received December 16, 1971

A tetragonal structural model for cationic vacancy ordering in the lanthanide sesquichalcogenides having the Th_3P_4 structure is developed from considerations involving the metal site stereohedra or Wigner–Seitz cells and tested by Madelung constant calculations. In addition the anion stereohedra are discussed as well as the Voronoi polyhedra for both metal and nonmetal sites. The electrostatic results include crystal potential calculations as a function of charge. Madelung constants and potentials were also calculated for charge ordering in semiconducting materials like Eu_3S_4 as a function of atomic position and c/a ratio. In these materials electrostatic stability is associated with increasing vacancy and charge ordering.

Introduction

The growing literature on rare earth compounds having the Th_3P_4 structure testifies to the great versatility of this high temperature phase in accommodating large quantities of metal site vacancies and cation substitutions. For the pure compounds the composition generally varies between R_2X_3 and R_3X_4 where R represents a light rare earth metal and X indicates either sulfur, selenium or tellurium (*1–4*). The R_2X_3 compositions in the Th_3P_4 structure are insulating or semiconducting and correspond to a vacancy concentration of 1/9 of the metal sites (*5*). When these vacancies are filled with trivalent metals such materials as Ce_3S_4, Gd_3Se_4, and Nd_3Te_4 are semimetallic and demonstrate no appreciable lattice parameter increase over those of the R_2X_3 or metal-poor composition. The vacancies in the R_2X_3 composition can also be wholly or partly filled with divalent alkaline earths (*4, 6–8*), divalent transition metals (*9*) or divalent lanthanides (*10*) with the maintenance of the semiconducting or insulating character of the R_2X_3 composition all the way to the filled structures including $CaCe_2S_4$, $SrGd_2Se_4$, $YbDy_2S_4$, Eu_3S_4, and Sm_3Se_4. In the latter two compounds semiconductivity is achieved by the localization of the itinerant electrons responsible for electrical conductivity in the trivalent compounds to give both trivalent and divalent Sm and Eu atoms in the ratio of 2:1 [see (*4*)]. Thus the versatility of the structure to accommodate a variety of substitutions and hence various electron/atom ratios, has encouraged many phase studies, especially by Flahaut and his coworkers, as well as many studies involving transport phenomena, such as thermoelectricity (*11, 12*), electron mobility control (*7, 8*), electron transport (*13, 14*), Mössbauer effects (*15, 16*), and superconductivity (*17*), as well as optical (*18*) and magnetic effects (*16, 19, 20*).

In the above compounds it is generally considered that the trivalent and divalent metals, as well as the vacancies, all occupy the same set of crystallographically equivalent sites on a purely statistical basis (*5*). This is in contrast to the situation involving the heavier rare earth chalcogenides where such compounds as $BaHo_2Se_4$ have the same orthorhombic structure type (*21*) as $CaFe_2O_4$ involving nonequivalent divalent and trivalent sites. As noted earlier (*7*), the assumption of only statistical occupancy is somewhat more extreme for the pure lanthanide and actinide sesquisulfides for which Zachariasen originally proposed that 1-1/3 vacancies are randomly distributed among the 12 metal sites. Since each metal atom has eight near-metal neighbors in the Th_3P_4 structure, the probability of the pairing of vacancies is sufficiently high (8/81) that pairing cannot be ignored in even a zero-order discussion. In addition, the absence of two large metal atoms associated with adjacent vacancies would lead to serious collapse of the structure in that area and would appear to be highly unlikely on the scale

called for by the statistics alone. Since the ordering of vacancies does not appear to have been discussed in the literature and since such ordering, if it exists, could have important ramifications in the single crystal properties of these materials, the question of vacancy and charge ordering (as in $Eu^{+2}Eu_2^{+3}S_4^{2-}$) is the subject of this paper.

The ordering of vacancies among the metal sites is first sought through the construction of the Voronoi space-filling polyhedra associated with the metal atoms only. Support for the various resultant models of vacancy ordering is next discussed through the assumption of an ionic model and the calculation of Madelung constants and Madelung potentials via the method of Bertaut (*22*, *23*) for structures with site occupancy disorder (*24*). Madelung potentials for the various ions are calculated in anticipation of their use in the interpretation of photoelectron spectroscopic studies of these materials. The effect of charge ordering on the pnictide (or chalcogen) position is then considered. In separate sections the stereohedra for the nonmetal sites are presented as well as the Voronoi polyhedra for the aggregate of metal and nonmetal P (phosphorus) sites. In the final section experimental evidence for charge and vacancy ordering is considered as well as some of the possible physical consequences of such ordering. The occurrence of ordering should increase interest in materials having the noncentrosymmetric Th_3P_4 structure since the possibilities for nonlinear optical and magnetic phenomena are expanded by the presence of the uniaxial tetragonal structures in this series of compounds of demonstrated versatility.

To close the introduction it is perhaps useful to consider the role of the Voronoi polyhedra in physical chemistry. Introduced by the mathematician G. Voronoi (*25*) in 1908, this polyhedron was the three-dimensional analogue of the Dirichlet region of a point in an array or aggregate of points. In a Voronoi polyhedron about a particular array point, all increments of space are closer to that point of the array than to any other point of the array. This concept has been employed by Bernal (*26*) in a treatment of the geometric structures of glass and by Smith (*27*) in a discussion of glass viscosity. The Voronoi polyhedra are termed "parallelohedra" when the array of points are related by translation symmetry only. However, when the array of points correspond to a single type of crystallographically equivalent points these space-filling Voronoi polyhedra are generally termed "stereohedra." In solid state physics such stereohedra are the well-known Wigner–Seitz cells when centrally occupied by an atom. In an interesting discussion of ionic structures Gorter (*28*) recently employed his SFP (space-filling polyhedra) in a useful classification of ionic crystal structures. These SFP are usually stereohedra; however, the vertices of these SFP can be partly occupied by atomic species different from the central occupant. In this paper Voronoi polyhedra are used to develop a chemically and electrostatically reasonable model of disorder. In addition, nonidentical Voronoi polyhedra are introduced for the Th_3P_4 structure corresponding to an aggregate consisting of both the metal and nonmetal sites.

The Vacancy Model[1]

In the search for a possible ordering of vacancies in the Ce_2S_3-type compounds having the Th_3P_4 structure it was quickly apparent that the chalcogen positions could and should be ignored in the first considerations. The relationship between the metal atoms is then revealed by the construction of the metal site stereohedra or Wigner–Seitz cell. These space-filling polyhedra are obtained as follows: The intersections of the planes which are the perpendicular bisectors of the interatomic metal–metal distances from a single metal site define a series of polyhedra of increasing volume. The smallest such polyhedron containing the central metal site is the desired one. For the Th_3P_4 structure one obtains dodecahedra with a volume of 1/12 the unit cell and which, when duplicated at each metal site with the correct orientation, fill all space. Each dodecahedron has eight identical faces which can be considered as obliquely truncated isosceles triangles associated with the nearest-neighbor metal–metal interactions and four additional isosceles triangles associated with the next-nearest metal–metal distances. These faces are arranged to give $\bar{4}$ symmetry to the polyhedra (see Fig. 1). By linking together through their triangular faces that set of dodecahedra corresponding to the next-nearest interactions only, one forms an open (but distorted) diamond-like structure (Fig. 2). In this structure of stereohedra all $\bar{4}$ axes of the dodecahedra are parallel to each other and to one of the cubic axes. There are three interpenetrating networks such that each metal site (or dode-

[1] These vacancy models were first presented at the Eighth Rare Earth Research Conference (*29*).

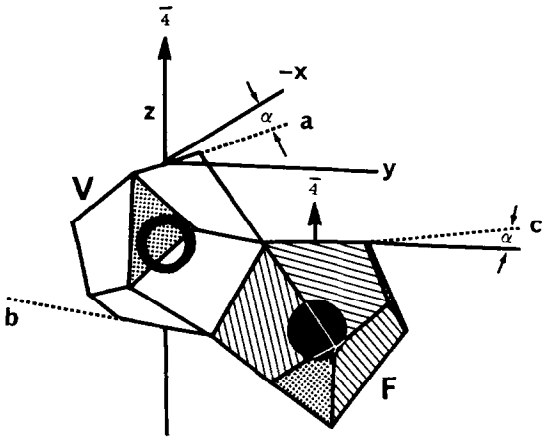

FIG. 1. Two of the space-filling dodecahedra corresponding to next-nearest metal neighbors in the Th_3P_4 structure are shown sharing a common triangular face. The stereohedral edges marked *a*, *b* and *c* are perpendicular to their $\bar{4}$ axes (the *z* direction) and make an angle of 26.56° with the [100] or [010] direction.

cahedron) has as nearest neighbors only those dodecahedra with their $\bar{4}$ axes perpendicular to its own. By randomly distributing the vacancies among the metal sites corresponding to just one of the diamond-like structures (called here, D_z) one obtains a tetragonal structure with the space group $I\bar{4}2d$–D_{2d}^{12} (No. 122). In such a case the vacancies are no nearer than second-nearest metal–metal neighbors and fourth-nearest neighbors including the metalloid atoms. This form of ordering gives the metal atom a shell of sixteen neighbors before it sees the metal atom shell containing vacancies.

Further ordering is obtained by restricting the vacancies to half the D_z sites. This results in a wurtzite-like structure in which each site *V* (for vacancy) is tetrahedrally surrounded by four *F* (filled) sites and vice-versa. This wurtzite-like structure with cell edges, A_w, B_w and C_w, has a severe tetragonal distortion such that $\sqrt{2}C_w = A_w = B_w = \sqrt{2}a_0$ where a_0 is the cubic unit cell edge. Now the vacancy sites (*V*) are only third-nearest metal–metal neighbors in a structure of even lower tetragonal symmetry (space group $I\bar{4}$–S_4^2, No 82). This structure is seen in Fig. 2 which shows neither the filled D_x or D_y metal sites nor the 16 metalloid positions.

The relation between the various space groups is indicated in Table I which shows the symmetry of the sites germane to the Th_3P_4 structure along with the approximate atomic parameters. The directions of further shifts in the metalloid positions are indicated by δ terms assuming zero metal shifts but an increased size for the occupants of the D_z sites. In calculating the approximate parameters we note that between the Th_3P_4 structure and the tetragonal space groups there is an origin shift of 0, 1/4, −1/8.

Three possible models for the ordering of vacancies in the rare earth sesquichalcogenides are now readily described.

(1) The vacancies can be distributed among the 12a positions of the Th_3P_4 structure which include the D_x, D_y, and D_z substructures. In agreement with Zachariasen's proposal (*5*), the probability of finding a vacancy in a metal site is 1/9 and the probability of finding two adjacent vacancies is 8/81.

(2) The vacancies are distributed among the 4a sites of the $I\bar{4}2d$–D_{2d}^{12} space group corresponding to the D_z sites only. The probability of finding a vacancy in such a site is 1/3 for the R_2X_3 compositions and vacancies are no closer than

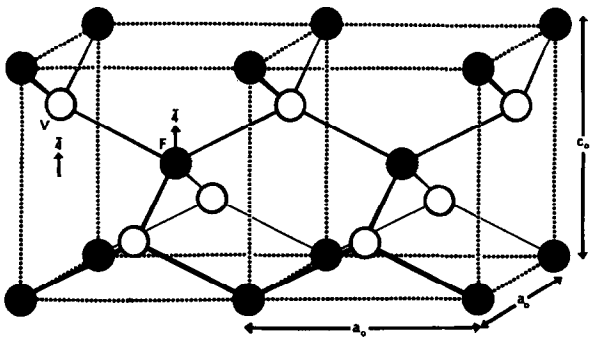

FIG. 2. The D_z substructure of the metal sites with $\bar{4}$ symmetry is illustrated for two unit cells with the relative positions of the sites marked *V* and *F* the same as in Fig. 1. A charge ordered structure proposed for Eu_3S_4 would have divalent metal atoms in both the *V* and *F* positions with the trivalent ions in the metal atom twofold positions (not shown) of space group No. 122.

TABLE I

BODY CENTERED TETRAGONAL STRUCTURES AND THEIR RELATION TO THE Th_3P_4 STRUCTURE

Space group	Position	Metal Site Symmetry	$u\ v\ w$[a,b]	Metalloid Site Position	Metalloid Site Symmetry	$u\ v\ w$[a,b]
$I\bar{4}3d$–T^6d No. 220 (Th_3P_4)	12a (D_x, D_y, D_z)	$\bar{4}$	$\frac{3}{8}\ 0\ \frac{1}{4}$	16c	3	$x\ x\ x$ $x \cong \frac{1}{12}$
$I\bar{4}2d$–D_{2d}^{12} No. 122	4a (D_z)	$\bar{4}$	$0\ 0\ 0$	16e	1	x, y, z
	8d (D_x, D_y)	2	$x\ \frac{1}{4}\ \frac{1}{8}$ $x \cong \frac{3}{8}$			$x \cong \frac{1}{12} - \delta$ $y \cong \frac{1}{3} + \delta$ $z \cong \frac{23}{24} - 2\delta$
$I\bar{4}$–S_4^2 No. 82	2a (F)	$\bar{4}$	$0\ 0\ 0$	8g	1	$x\ y\ z$
	2c (V)	$\bar{4}$	$0\ \frac{1}{2}\ \frac{1}{4}$			$x \cong \frac{1}{12} - \delta$ $y \cong \frac{1}{3} + \delta$ $z \cong \frac{23}{24} - 2\delta$
	8g (D_x, D_y)	1	$x\ y\ z$ $x \cong \frac{3}{8}$ $y \cong \frac{1}{4}$ $z \cong \frac{1}{8}$	8g′	1	$x'\ y'\ z'$ $x' \cong \frac{1}{12} - \delta$ $y' \cong \frac{1}{6} - \delta$ $z' \cong \frac{7}{24} + 2\delta$

[a] Typical atomic parameters are given; equivalent positions are obtained from the unit cell symmetry elements.

[b] When δ equals zero both Th and P type atoms are in the filled Th_3P_4 structure with $x(P) = 1/12$. The shift δ (positive) is for large atoms on the D_z sites.

second-nearest metal neighbors. This would appear to be a reasonable model for the sesquisulfides, as usually prepared, as well as for charge ordered semiconductors like Eu_3S_4 at low temperature.

(3) By restricting vacancies to just one of the $\bar{4}$ sites in the $I\bar{4}$–S_4^2 structure the probability of the site being vacant is 2/3; now vacancies are no closer than the third-nearest metal neighbors. In the figures the site selected is the 2c or V site. Such ordering might occur for a well-annealed sesquisulfide. These examples are included in

TABLE II

POSSIBLE ORDERED SEMICONDUCTING COMPOUNDS BASED ON Th_3P_4-TYPE STRUCTURES

Entry No.	Compound	Metal sites: D_z F	Metal sites: D_z V	Metal sites: D_x, D_y	Space Group No.	Position Fig. 3
1	Ce_2S_3	($\frac{8}{9}Ce^{3+}$, $\frac{1}{9}\square$)	($\frac{8}{9}Ce^{3+}$, $\frac{1}{9}\square$)	($\frac{8}{9}Ce^{3+}$, $\frac{1}{9}\square$)	220	A
2	Ce_2S_3	($\frac{2}{3}Ce^{3+}$, $\frac{1}{3}\square$)	($\frac{2}{3}Ce^{3+}$, $\frac{1}{3}\square$)	Ce^{3+}	122	B
3	Ce_2S_3	Ce^{3+}	($\frac{1}{3}Ce^{3+}$, $\frac{2}{3}$)	Ce^{3+}	82	C, C′
4	Sm_3S_4	Sm^{2+}	Sm^{2+}	Sm^{3+}	122	B
5	$EuGd_2Se_4$	Eu^{2+}	Eu^{2+}	Gd^{3+}	122	B
6	$FeBaLa_4Te_8$	Fe^{2+}	Ba^{2+}	La^{3+}	82	B
7	$Th_5P_4S_4$	Th^{4+}	□	Th^{4+}	82[a]	D, D′
8	$MnBaTh_4P_4S_4$	Mn^{2+}	Ba^{2+}	Th^{4+}	82[a]	E
9	$KFeCe_4S_8$	K^{1+}	Fe^{3+}	Ce^{3+}	82	C, C′
10	$TiCe_4Se_8$	Ti^{4+}	□	Ce^{3+}	82	F, F′

[a] Nonequivalent metalloid atoms are permitted in space group No. 82.

Table II along with other possible new semiconducting compounds based on the Th_3P_4 type structure. Note that some of these suggest the possibility of both *n*- and *p*-type conductivity with suitable cationic doping. Reports of the latter type conductivity are rare (*2*).

Electrostatic Energy Calculations

Support for the above model of vacancy ordering will be presented from the results of Madelung constant calculations. However, first it is appropriate to discuss three points pertinent to the method and to the structure of interest.

(1) In the treatment of disordered cations or vacancies it is usually assumed that an average charge can be associated with the site of disorder in a Madelung constant calculation. Using the method of Bertaut (*22*, *23*), Brunel and de Bergevin (*24*) have recently shown that this assumption is correct for total disorder but that the calculation must be modified if partial ordering is present. The cases treated here will be those of total disorder.

(2) While it is unlikely that any material possessing the Th_3P_4 structure is either wholly ionic or wholly covalent (or metallic) in nature, for the purposes of this paper an ionic model seems appropriate for the rare earth chalcogenides. This is in line with the recommendation of Gorter (*28*), who suggests that even for materials of appreciable covalency, an ionic representation has utility in energy considerations.

(3) The final point concerns the question of the appropriate position parameters to use for the metalloid atom or chalcogen. While Zachariasen (*5*) originally suggested the value of $x = 1/12$ (0.083), this was predicted by the author to be too large on the basis of both electrostatic energy and covalent bond considerations (*1*, *30*). This prediction has since been experimentally verified by Holtzberg, Okaya, and Stemple (*31*) for the compounds La_3Se_4 ($x = 0.075$) and Ge_2Se_3 ($x = 0.0715$), by Cox, Steinfink, and Bradley (*32*) for La_2Te_3 ($x = 0.075$), and by Virkar, Singh, and Roman (*33*) for the anti-Th_3P_4 structure of $La_4Rh_{\sim 3}$ ($x = 0.057$) Accordingly, the following electrostatic energy calculations have been made with $x = 1/14$ (0.0714) as a reasonable and useful approximation.

The electrostatic energy calculations and the crystal potentials were obtained using the method of Bertaut (*22*, *23*) and the average charge for disordered sites (*24*). Using the notation of Templeton (*34*, *35*), for j atoms per unit cell we have

$$A = -\frac{WL}{\epsilon^2} = \frac{gL}{RN}\sum_j z_j^2 - \frac{\pi R^2 L}{NV}\sum_{h_i} F^2\Phi(\alpha)/h^2 \tag{1}$$

where A is the Madelung constant, W is the electrostatic energy, ϵ is the electron charge, N is the number of molecules in the unit cell, z_j is charge number of the atom j, h is the magnitude of the reciprocal lattice vector $(h_1 h_2 h_3)$ and F is the structure factor term of Eq. (2).

$$F = \sum_j z_j \exp\left[2\pi i(h_1 x_1 + h_2 x_2 + h_3 x_3)\right]. \tag{2}$$

The function $\Phi(\alpha)$ is equal to the square of the Fourier transform of the spherical charge distribution $f(r)$ of atom j at coordinates $(x_1 x_2 x_3)$. In this paper the charge distribution $f(r)$ is given by Eq. (3)

$$f(r)\begin{cases} = 3(R-r)/\pi R^4 & r \leqslant R \\ = 0 & r > R, \end{cases} \tag{3}$$

where R is the effective sphere radius and the corresponding self-energy factor g, is $=26/35$. The parameter α is simply $2\pi hR$ and L is taken as the cube root of the unit cell volume.

The potential V_j at the site of the j atom is given (*23*) by $V_j = \partial W/\partial z_j$ and may be simply related to the total electrostatic energy W by a sum over all j atoms; as in Eq. (4).

$$W = \tfrac{1}{2}\sum_j V_j z_j. \tag{4}$$

While in a few simple binary structures the potentials V_j may be readily calculated from the Madelung constants alone using symmetry relations, this is not possible in general. On the other hand, using the method of Bertaut, the potentials are readily calculated at the same time as the Madelung constant. In view of the increasing interest in the compounds having the Th_3P_4 structure and the demonstrated need for the Madelung potentials in the interpretation (*36*, *37*) of photoelectron spectroscopy (ESCA) the potentials for compounds having the Th_3P_4 structure are also reported here.

Results. In Tables III and IV the Madelung constant (A) and the Madelung potentials ($V_j L/\epsilon$) are presented for the various metal and metalloid sites of space group No. 84 ($I\bar{4}$–S_4^2) with a metalloid site charge of −0.75 at both positions 8g and 8g′ of Table I, with an average cation charge of +1.00, with $x = 1/14$, and with a c/a ratio of 1.0. The labels of the columns, R_V, and

TABLE III

MADELUNG CONSTANTS FOR Th_3P_4 TYPE STRUCTURES AS A FUNCTION OF CATION CHARGE

R_V =	0.0	0.1	0.2	0.3	0.4	0.5	0.6	0.7	0.8	0.9	1.0	R_F
	59.1049	58.5572	58.0874	57.6953	57.3810	57.1445	56.9858	56.9048	56.9016	56.9762	57.1286	2.0
0.0	62.9304	57.9905	57.5015	57.0903	56.7569	56.5012	56.3233	56.2233	56.2010	56.2564	56.3897	1.9
0.1	62.0002	61.0892	56.9934	56.5630	56.2105	55.9357	55.7387	55.6195	55.5781	55.6144	55.7286	1.8
0.2	61.1478	60.2559	59.4417	56.1136	55.7419	55.4480	55.2319	55.0935	55.0330	55.0502	55.1452	1.7
0.3	60.3732	59.5004	58.7053	57.9881	55.3511	55.0381	54.8028	54.6453	54.5657	54.5638	54.6396	1.6
0.4	59.6763	58.8227	58.0468	57.3486	56.7283	54.7059	54.4515	54.2749	54.1761	54.1551	54.2119	1.5
0.5	59.0573	58.2227	57.4659	56.7869	56.1857	55.6623	54.1780	53.9823	53.8644	53.8242	53.8618	1.4
0.6	58.5160	57.7005	56.9629	56.3030	55.7210	55.2167	54.7901	53.7675	53.6304	53.5711	53.5896	1.3
0.7	58.0525	57.2562	56.5376	55.8969	55.3340	54.8488	54.4414	54.1118	53.4742	53.3958	53.3952	1.2
0.8	57.6667	56.8896	56.1902	55.5686	55.0247	54.5587	54.1704	53.8599	53.6272	53.2982	53.2785	1.1
0.9	57.3588	56.6007	55.9205	55.3180	54.7933	54.3463	53.9772	53.6859	53.4723	53.3365	53.2396	1.0
1.0	57.1286	56.3897	55.7286	55.1452	54.6396	54.2119	53.8618	53.5896	53.3952	53.2785	53.2396	
R_V =	0.0	0.1	0.2	0.3	0.4	0.5	0.6	0.7	0.8	0.9	1.0	

the rows R_F are defined in terms of the average cationic charge z_{ac} by Eq. (5)

$$R_V = z_V/z_{ac}$$
$$R_F = z_F/z_{ac} \qquad (5)$$
$$z_D = (6\,z_{ac} - z_F - z_V)/4$$

TABLE IV

MADELUNG POTENTIALS AS A FUNCTION OF CHARGE FOR $c/a = 1.0$

Notation		Coefficients		
Crystallographic[a]	This paper	b_0 Constant	b_F R_F	b_V R_V
Metal				
2a	F	−1.80751	−3.08145	−0.14882
2c	V	−1.80751	−0.14882	−3.08145
8g	D_x, D_z	−6.65292	+0.80757	+0.80757
Metalloid				
8g		+3.83549	+0.05999	−0.05999
8g′		+3.83549	−0.05999	+0.05999

[a] Space group $I\bar{4}$–S_4^2, No. 82.

where z_V is the average charge associated with the V or vacant metal site 2a, z_F is the charge of the F site 2c, and z_D is the charge of the metal atom at D_x, D_y sites, 8g. The calculated Madelung potentials may be expressed using Eq. (6)

$$V_j L/\epsilon = b_0 + b_F R_F + b_V R_V \qquad (6)$$

for the condition that the metalloid sites 8g and 8g′ are the same from a coordination and bond distance point of view. Under this condition we note from the linearity of Eq. (6) and coefficients given in Table IV that the crystal potential for the metal atom at site 2c is the transpose of that for the metal atom at site 2a and that a similar relation obtains for the metalloid atoms at sites 8g and 8g′. All calculations were made for the charge distribution radius R, Eq. (3), equal to 15% of the a_0 unit cell edge and to a maximum value of $\alpha = 3\pi$: the self-consistency was checked using Eq. (4). The correction to the Madelung constant suggested by Templeton (*34*) has not been applied due to its smallness (0.1% of the Madelung constant) and the uncertainty in its proportioning among the crystal potenials of the various atoms.[2]

The general correctness of these results were further checked against the "reduced Madelung constant" of Templeton (*38*, *39*) defined by Eq. (7),

$$\alpha_R = 2A(R_0)/\sum_j z_j^2 \qquad (7)$$

[2] It appears probable that the correction should be proportioned among the atoms j according to their charges as $2z_j/\Sigma_j z_j^2$ with the sign of the correction chosen according to the sign of the charge.

where $A(R_0)$ is the Madelung constant based on the smallest cation–anion distance (R_0) and the sum is taken over all atoms in the unit cell. For the Th_3P_4 structure with $x = 1/14$ and $R_V = R_C = 1.0$, then the reduced Madelung constant, using Table III, is $\alpha_R = 1.691$. Templeton has also shown that α_R may be approximated by Eq. (8) where m is the

$$\alpha_R = 1.89 - 1.0/m \tag{8}$$

weighted harmonic means of the coordination number. For the Th_3P_4 structure $m = 6.72$ and substitution in Eq. (8) yields a value of $\alpha_R = 1.74$, in reasonable agreement with the accurate calculated value of 1.691. Of greater importance is the linearity of the Madelung potentials with charge (R_F and R_V) as indicated by the computed results summarized in Table IV. This gives considerable support to Templeton's argument that the charges of the ions in ternary and more complex systems should enter as the square in the formula for the reduced Madelung constant [Eq. (7)].

Contours of constant Madelung constant are shown in Fig 3 based on the contents of the cubic unit cell with the metalloid parameter of $x = 1/14$ and the two anion charges equal to -0.75. The contours are a function of cation charge ratios R_F and R_V [Eq. (5)] and show mirror plane symmetry along the diagonals of Fig. 3. This mirror symmetry is independent of the x parameter and may be used in conjunction with Table III to obtain the Madelung constant in the range R_F, $R_V = 0.0$ to 2.0. However, we note that this high symmetry would disappear if chemically different metalloid atoms occupied the 8g and 8g′ sites. While the Madelung map has been calculated only for R_F, $R_V \leqslant 2.0$, there is no reason for this upper limit beyond the practical one that few compounds will correspond to the picture with R_F, $R_V \leqslant 2.0$.

In order to see the effect of vacancy or charge ordering on specific examples it is useful to relate particular entries of Table II to their position on the contour map of Fig. 3. Electrostatically the least stable position is indicated by the energy minimum in Fig. 3 at position A which corresponds to complete cationic (or vacancy) disorder as in Ce_2S_3, entry 1 of Table II. By restricting the vacancy disorder in Ce_2S_3 to just the D_z sites, as in entry 2, we see that the structure is electrostatically more stable, position B. This position, B, also corresponds to charge ordering in Eu_3S_4 and Sm_3S_4, entry 4, and to cationic ordering in entry 5, $EuGd_2Se_4$, and cationic ordering according to valence in entry 6. If the vacancies in Ce_2S_3 are restricted to just the

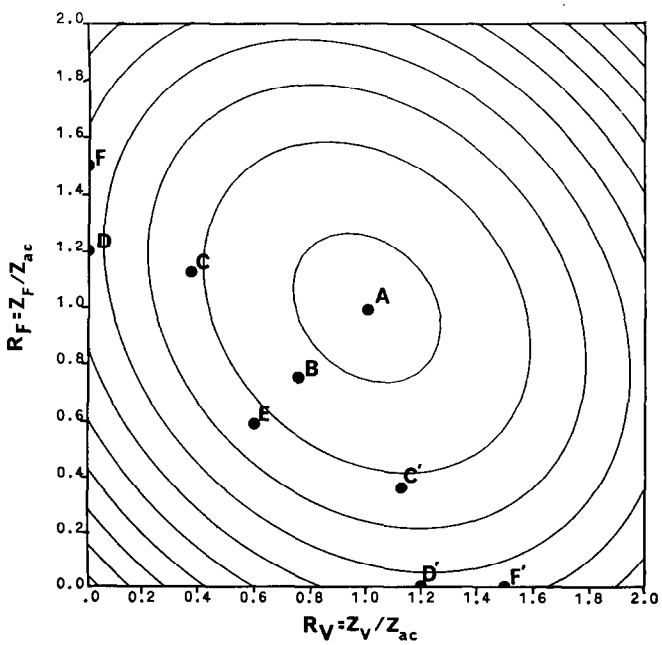

FIG. 3. A Madelung constant contour map is shown for the Th_3P_4 structure as a function of the ratio of charges of the cations at the F and V sites to the average cationic charge z_{ac}. Here the c/a ratio is 1.0 and the metalloid parameter is $x = 1/14$. The contour intervals are $1.0/\epsilon^2$ apart increasing from the central least stable contour of $53.5/\epsilon^2$.

V sites, entry 3, Table II, then the structure is further stabilized by the shift from position B to position C. An example of cationic ordering at position C is suggested by entry 9 while a related example of both cationic and vacancy ordering is indicated by $TiCe_4Se_8$, entry 10, at the even more stable location, position F. The hypothesized vacancy ordered compound $Th_5P_4S_4$, entry 7 and position D, and cationic ordered compound $MnBaTh_4P_4S_4$, entry 8 and position E, should not really be indicated on the contour map unless either there is complete metalloid disorder between phosphorus and sulfur or the effective charges of the anions are equal and their positions are equivalent (unlikely). Similarly it is to be expected that the effective charges of divalent Fe and Ba in a compound like $FeBaLa_4Te_8$, entry 6, will not be equal; hence, position B for this compound represents an idealization. Finally we note that compounds which correspond to positions like D and F will most likely be obtained in the ordered state if they can be prepared.

Effect of c/a and position variations. The ordering of charges in materials like Eu_3S_4 and Sm_3S_4 (Table II, No. 4) is expected to result in a tetragonal structure. Accordingly, the Madelung constant, Table V, and the Madelung potentials, Table VI, have been calculated for these materials in the charge ordered state ($R_V = R_F = 0.75$) as a function of *c/a* and the metalloid shift parameter δ in the tetragonal space group, $I\bar{4}2d$-D_{2d}^{12}. The use of δ, as defined below, is a single parameter approximation which takes into account the increased size of the divalent cations when occupying the D_z (4a) sites. The four parameters indicated in Table I for this space group, No. 122, are reduced to one as follows: the metal D_x, D_y parameter, x, is taken as 3/8, that is, its cubic Th_3P_4 value. The metalloid position (x,y,z) is also related to its cubic Th_3P_4 location by Eq. 9,

$$\begin{aligned} x &= x' + \delta x \\ y &= x' + \tfrac{1}{4} + \delta y \\ z &= x' - \tfrac{1}{8} + \delta z \end{aligned} \tag{9}$$

where x' is the P site parameter in the space group No. 220 and where δx, δy, and δz are our adjustable parameters. The eight metalloid positions about the metal atom in cubic Th_3P_4 have been described (*7*, *19*) as the sum of two metalloid tetrahedra, a flat tetrahedron of four nonmetals which are almost in a plane perpendicular to the $\bar{4}$ axis and a long narrow tetrahedron of nonmetals at somewhat greater distances experimentally. Now if we keep the more important flat tetrahedral distances (two) equal for the trivalent cation (8d site) in the charge-ordered phase of Eu_3S_4 then we obtain the relationship of Eq. (10). If the flat tetrahedral distances

$$0 = 3\delta x - \delta y - 2\delta z \tag{10}$$

$$0 = 2\delta y + \delta z \tag{11}$$

are made equal to the long tetrahedral distances for the divalent metal in the 4a site with $x' = 1/12$, then Eq. (11) is obtained. These two restrictions combine to give the single parameter δ as in Eq. (12).

$$\delta = \delta y = -\delta x = -\tfrac{1}{2}\delta z \tag{12}$$

For δ positive and increasing; (1) the eight Eu–S distances for divalent europium increase but remain equal, (2) the four flat tetrahedral Eu–S distances for trivalent europium decrease and remain equal, (3) two of the long tetrahedral distances of trivalent europium decrease while

TABLE V

MADELUNG CONSTANTS FOR *c/a* VS. METALLOID SHIFT, δ, IN CHARGE ORDERED COMPOUNDS[a]

	$\delta =$					
c/a	0.000	0.005	0.010	0.015	0.020	0.025
0.96	54.9157	55.2236	55.4427	55.5540	55.5316	55.3425
0.98	54.1897	54.4842	54.6959	54.8054	54.7864	54.6056
1.00	53.4794	53.7612	53.9657	54.0735	54.0580	53.8854
1.02	52.7840	53.0536	53.2514	53.3578	53.3458	53.1812
1.04	52.1027	52.3606	52.5521	52.6573	52.6489	52.4923
1.06	51.4350	51.6819	51.8675	51.9718	51.9671	51.8185

[a] Space group $I\bar{4}d$-D_{2d}^{12}, No. 122.

TABLE VI

MADELUNG POTENTIALS FOR THE THREE POSITIONS IN CHARGE ORDERED COMPOUNDS[a]

		δ =					
c/a	Site	0.000	0.005	0.010	0.015	0.020	0.025
0.96	4a(D_z)	−4.3173	−4.1508	−3.9808	−3.8094	−3.6381	−3.4686
	8d(D_x, D_y)	−5.5785	−5.6693	−5.7711	−5.8823	−6.0014	−6.1265
	16e	3.8894	3.9143	3.9169	3.8949	3.8447	3.7617
0.98	4a	−4.2660	−4.0950	−3.9208	−3.7454	−3.5705	−3.3976
	8d	−5.5018	−5.5938	−5.6971	−5.8103	−5.9315	−6.0590
	16e	3.8387	3.8616	3.8629	3.8402	3.7899	3.7073
1.00	4a	−4.2156	−4.0403	−3.8622	−3.6831	−3.5048	−3.3289
	8d	−5.4269	−5.5200	−5.6248	−5.7397	−5.8629	−5.9927
	16e	3.7892	3.8101	3.8101	3.7867	3.7363	3.6541
1.02	4a	−4.1659	−3.9867	−3.8049	−3.6224	−3.4410	−3.2622
	8d	−5.3537	−5.4479	−5.5540	−5.6706	−5.7957	−5.9277
	16e	3.7406	3.7597	3.7585	3.7345	3.6839	3.6022
1.04	4a	−4.1169	−3.9341	−3.7489	−3.5632	−3.3789	−3.1976
	8d	−5.2819	−5.3772	−5.4847	−5.6028	−5.7298	−5.8638
	16e	3.6931	3.7104	3.7080	3.6833	3.6327	3.5515
1.06	4a	−4.0688	−3.8826	−3.6942	−3.5056	−3.3186	−3.1348
	8d	−5.2117	−5.3080	−5.4168	−5.5364	−5.6652	−5.8012
	16e	3.6465	3.6620	3.6585	3.6333	3.5827	3.5019

[a] Space group $I\bar{4}2d$–D_{2d}^{12}, No. 122.

two increase, and (4) two of the three short metalloid–metalloid distances increase while one decreases. When δ is approximately 0.020 the distances appear reasonable for Eu_3S_4 with the exception of the one short metalloid–metalloid interaction which remains nonbonding but is too short for either a S–S van der Waals interaction or an anion interaction. In the real structure this short distance is probably removed by the variation of x parameter of the metal atom and the relaxation of the restriction of Eq. 12.

As c/a increases we see from Table V that charge ordering becomes decreasingly stable. However, an increase in δ gives an initial increase in electrostatic stability. Such an increase might be expected as the metalloid moves away from the larger divalent cation to the more numerous and more highly charged trivalent cation. It is reasonable to expect that the one parameter model using δ underestimates this effect since the short metalloid–metalloid distance decreases the Madelung constant. The decrease in the Madelung constant for δ greater than 0.015 is probably due to this short metalloid–metalloid distance. Even so Table V indicates that a δ of 0.020 more than compensates for a c/a increase of 0.015 in terms of electrostatic stability.

Ordering and the Chalcogen Site

While the rare earth metal in the chalcogenides having the Th_3P_4 structure has a coordination of eight in the form of two interpenetrating tetrahedra, the chalcogen atom sits on the threefold axis of a twisted trigonal prism of six metal atoms. In cubic Th_3P_4 the chalcogen coordinates are x, x, x where x is $<1/12$ experimentally. As x decreases it moves toward the bottom triangle of the twisted prism and shortens the distances corresponding to the flat tetrahedra about the metal site while lengthening the chalcogen–metal distances of the top triangle corresponding to the long tetrahedra.

If the semiconducting Sm_3S_4 compound were to have an ordered structure with the divalent ions in the D_z sites (4a positions of the $I\bar{4}2d$–D_{2d}^{12} space group) then each sulfur atom would be adjacent to two Sm^{+2} ions, one each in the

triangular base and top of the trigonal prism. The cation arrangement would distort the threefold symmetry of the sulfur atom as indicated in the section above; however, crystallographically there is still only one kind of metalloid in the ordered tetragonal Sm_3S_4 structure, that is the 16*e* position for the space group in Table I.

If, for the sesquisulfides, the vacancies were statistically distributed over all the D_z sites, the above discussion for Sm_3S_4 would be applicable; if however, they were restricted to the *V* sites then two-thirds of these metal positions would be vacant. If the vacancies were random among the *V* sites, then the $I\bar{4}$–S_4^2 space group would apply and there would be equal numbers of two different kinds of sulfur atoms, with the vacancy in either the base or top triangle of metal sites. Going beyond Table I and ordering the vacancies in the *V* positions so that every third *V* site along a stack of trigonal prisms ([111] direction in Th_3P_4) is now occupied by a metal atom, then there are six kinds of chalcogens, four of them with five metal neighbors and two of them with six neighbors. Other differences between them involve their distance from an occupied *V* site and whether the vacant *V* site is in the top triangle (long tetrahedra) or in the bottom triangle (flat tetrahedra). For the originally proposed (*5*) statistically distributed vacancies in Ce_2S_3 there are a large number of various kinds of S atoms, with fair fraction of them (16/81) having a pair of vacancies in a single triangular base.

For the sake of completeness we will describe in the next two sections the P site stereohedron and the Voronoi polyhedra before considering the experimental evidence for vacancy and charge ordering. These descriptions involving space-filling polyhedra are not only interesting in their own light but also provide new and useful insights into the Th_3P_4 structure.

P-Site Stereohedra

Earlier it was noted by the author (*7*) that the metalloid atoms in the Th_3P_4 structure could be linked by their shortest interaction distance to form two completely independent but interwoven networks. In the tetragonal $I\bar{4}$–S_4^2 space group, these independent networks are not equivalent and correspond, respectively, to the 8g and 8g′ metalloid sites (Table I). In the Th_3P_4 structure this difference between the networks is indicated by the fact that the stereohedra corresponding to the two different networks are enantiomorphically related.

In the Th_3P_4 structure the *P* site stereohedron for $x = 1/14$ is the trigonal hendecahedron illustrated in Fig. 4. The equilateral triangular faces[3] numbered 1 and 2 correspond to the second smallest metalloid–metalloid distance, i.e., interactions along the body diagonals to the stereohedron of the other network. The largest quadrilaterals, numbered 3–5 are bilaterally symmetric and correspond to the shortest interaction (absolute) between members of the same network. The two remaining sets of trigonally-related quadrilaterals numbered 6–8 and 9–11 in Fig. 4

[3] Close examination of Fig. 4 will show to the reader that the faces numbered 1 and 2 are not congruent as is required by the space-filling properties of the stereohedra. The three very small edges in the hexagonal face number 1 are taken to be a computing round-off error or a minor programming bug.

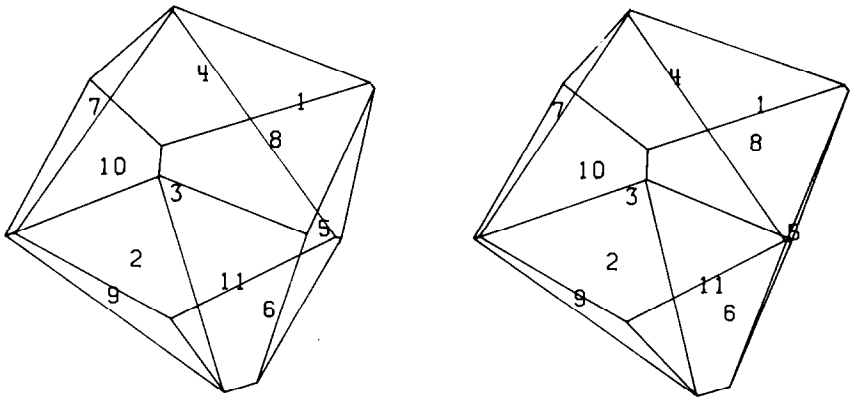

FIG. 4. The stereohedron for the metalloid or *P* site ($x = 1/14$) has been drawn for stereoscopic viewing. The *xz* plane is parallel to the plane of the paper with the *z* axis vertical. The parallel equilateral triangles numbered 1 and 2 are perpendicular to the [111] direction.

are congruent in shape and correspond to the interaction between one stereohedron and the enantiomorphic stereohedra of the other network. The relationship of these enantiomorphic stereohedra is such that a number 6 face of one is the number 9, 10, or 11 face of the other. As the P parameter x approaches 1/12, the shortest side in these quadrilateral faces disappears and the related vertices correspond to the meeting of five faces. When $x = 1/12$ these faces become isosceles triangles.

It is interesting to examine the stereohedron for $x = 1/12$ in its relation to the metal (Th) sites and the SFP of Gorter (*28*). This P site polyhedron ($x = 1/12$) has nine vertices which are divided into three groups, corresponding to the meeting of three, four, and five faces, respectively. The six vertices corresponding to the join of four and five faces are sites occupied by the metal atoms while no metal site is located at the join of three faces. In this case then the stereohedron is very similar to the SFP of Gorter. However, as x varies away from the value 1/12, only the three vertices corresponding to the meeting of three faces remains fixed in space. In Fig. 4 such a vertex is common to the faces numbered 3, 6, and 9. The remaining old vertices, as well as the new ones generated when x varies from the value 1/12, no longer correspond to the metal site locations. Hence it is important to note that either the useful SFP of Gorter are not in general stereohedra or that the metal (metalloid) sites are not generally located at the SFP vertices.

The Voronoi Polyhedra for the Th_3P_4 Structure

When the aggregate of points in a crystal is the sum of points at two or more different crystallographic sites then the more general term, Voronoi polyhedra, is appropriate for the smallest convex cells formed by the planes which perpendicularly bisect the intersite distances. In the Th_3P_4 structure there are three such Voronoi polyhedra forms which, together, fill all space One corresponds to the Th site and the other two are an enantiomorphic pair corresponding to the two networks of P sites.

The metal site cell is the hexadecahedron with 28 vertices shown in the stereograph, Fig. 5, for $x = 1/14$. The $\bar{4}$ symmetry of the site requires that there are only four different kinds of polygon faces. These faces are sequenced by size and the operations of the vertical $\bar{4}$ axis. The largest face shown, the octagons numbered 1–4, correspond to the shortest distance in the structure with $x = 1/14$, that is to the four metalloids arranged in a flat tetrahedron about the metal site. The second largest faces, the heptagons numbered 5–8, correspond to the four metalloids forming a long tetrahedron about the metal site. The remaining triangular polygons of much smaller area indicate the eight smallest metal–metal distances.

The P site enantiomorphic Voronoi polyhedra are trigonal heptadecahedra with 27 vertices, each of which is formed by the meeting of three faces. The six metal neighbors about the P site atom form a twisted trigonal prism in which the metalloid atom is only centered in the trigonal prism for the parameter $x = 1/12$. In Fig. 6 we see that corresponding to these six metal neighbors one has the large octagon faces 3–5 and the heptagons 6–8. The remaining faces are due to metalloid–metalloid distances.

The three largest of these faces, numbered 9–11, are bilaterally symmetric pentagons correspond-

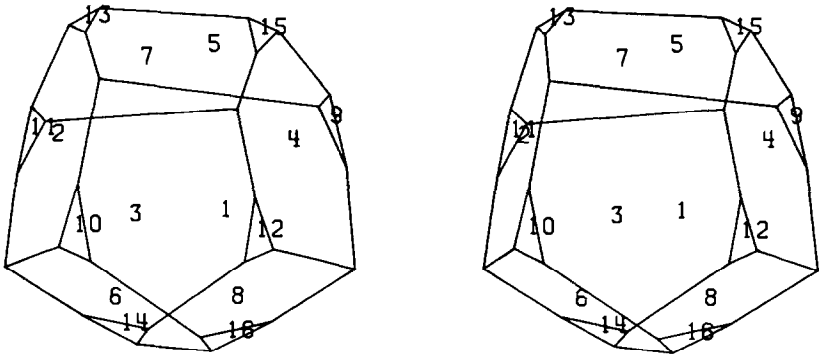

FIG. 5. The Voronoi polyhedron for the metal site is shown for the Th_3P_4 structure with the plane of the paper being the xz plane. The $\bar{4}$ axis is parallel to the vertical z axis and perpendicularly bisects the top edge joining faces 5 and 7. The smallest eight faces correspond to closest metal–metal interaction.

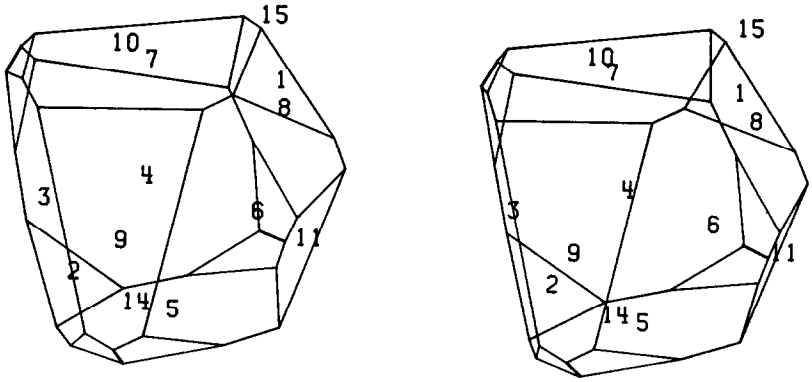

FIG. 6. This similarly oriented metalloid Voronoi polyhedron ($x = 1/14$) and its enantiomorph are the companions to that of Fig. 5. Together they fill all space. The triangular faces numbered 1 and 2 correspond to the second smallest metalloid–metalloid distance, an interaction which is along the [111] direction.

ing to the meeting of the congruent Voronoi metalloid polyhedra of the same network. Of course these faces are related to and are in the same plane as the bilaterally symmetric faces of the P site stereohedron in Fig. 4. In both cases, Figs. 4 and 6, it is interesting to note that the three axes of symmetry in these bilaterally symmetric faces are orthogonal, parallel to the x, y, and z axes, and constitute the $\bar{4}$ axes through the metal polyhedra. The equilateral triangular faces, numbers 1 and 2, are the common faces between cells of different networks along the unit cell body diagonal. The remaining six pentagonal faces, unnumbered, are congruent and are shared by P site polyhedra of different networks.

In examining the relationship of the eight nearest metalloid Voronoi polyhedra about a metal Voronoi polyhedron we find that each metal polyhedron has about it four P site polyhedra of each network. Each set of four are almost coplanar and are joined by their bilaterally symmetric faces to form a half circle which is centered on the $\bar{4}$ axis of the metal site.

Finally we note that the number of faces for both of the stereohedra, as well as for the Voronoi polyhedra above, are easily less than the maximum number, $14 + 8(h - 1)$, predicted by Delone (*41*) for stereohedra in a three-dimensional lattice involving a rotational group of order h.

Experimental Evidence for Ordering

The experimental evidence for the ordering of vacancies or charge in the Th_3P_4 structure is rather meager. The author knows of no lattice parameter or single crystal X-ray studies suggesting vacancy ordering. The observation of vacancy ordering would appear to be most likely in the light rare earth sesquisulfides grown at the lowest possible temperature. Although we have grown crystals (*42*) of Ce_2S_3 by iodine transport at 925°C, the small size of the crystals (less than 0.1 mm) prevented a definitive study. However, there were no obvious intensity or space group violations of the Th_3P_4 structure. On the other hand the refractory nature of these materials and the lack of lattice parameter variations from cubicity suggest that the single crystal could have an equal number of tetragonal domains with their c axes distributed along the "pseudo" cubic-cell edges. A very careful X-ray study involving statistical analysis of equivalent reflections may be required and/or disorder studies may be indicated.

The case for charge ordering is more encouraging than for vacancy ordering. Recent transport studies in bulk Eu_3S_4 provide some evidence for charge ordering in these semiconducting compounds. The presence of localized tri- and divalent cations in the ratio of 2:1 in samarium and europium chalcogenides with the Th_3P_4 structure has long since been established by magnetic susceptibility measurements and by their semiconducting properties. Mössbauer studies (*15*) in 1967 by Berkooz, Malamud, and Shtrikman show the existence of Eu^{3+} and Eu^{2+} ions in the expected ratio below 210°K but above that temperature the isomer-shift peaks broaden and then merge into a single intermediate peak consistent with a hopping electron transport model involving the Eu^{2+} "extra" electron. In the same material, Bransky, Tallan, and Hed have

observed (*43*) an electrical transition near 175°K as an abrupt change in activation energy from 0.16 to 0.21 eV, in reasonable agreement with 0.24 eV obtained by Berkooz et al. More recently Davis, Bransky, and Tallan (*44*) have shown from differential thermal analysis, magnetic data, and X-ray diffractometer tracings that a definite phase transformation occurs at 168°K and that it is nonmagnetic in origin. While their X-ray data is not definitive they have tentatively interpreted it on the basis of a tetragonal transformation with a c/a ratio of 1.004. From the calculated data presented in this paper it is reasonably clear that the small Madelung constant change of c/a associated with the transformation is more than compensated for by the effect of simple charge ordering (Table III) as well as by atomic movement associated with size effects (Table V). Accordingly, the observed phase transformation of Eu_3S_4 at 168°K is interpreted as a charge order–disorder transformation.

Such phase transformations should be observable by other experimental techniques. The loss of symmetry from $\bar{4}$- to 2-fold or to none in two-thirds of the metal sites suggests that the observation of charge or vacancy ordering might be possible via EPR, optical, or NMR experiments on single crystals. However, the local distortions from $\bar{4}$ symmetry may be rather small. On the other hand, the effect on the chalcogen is appreciable. For example, in the disordered Zachariasen Th_3P_4 structure there would be many kinds of S in Eu_3S_4, corresponding to the various combinations of distributing Eu^{3+} and Eu^{2+} ions at the corners of a twisted trigonal prism. In the ordered structure, at low temperature, only one kind of sulfur is present as indicated in Table I. Definitive single crystal X-ray support for vacancy ordering in the Th_3P_4 structures may be long in coming since an averaging process over different axis orientations may be unavoidable. Accordingly, other methods of detecting local site symmetry changes are highly recommended.

Summary

In concluding this paper we note that models for vacancy and charge ordering in rare earth compounds having the Th_3P_4 type structure have been derived from considerations involving the metal site space-filling stereohedra. It was further shown that these models have been supported by the calculations of Madelung constants and, for charge ordering in Eu_3S_4, by experimental data from the literature. In addition, a description of the metalloid site stereohedron has been given along with the Voronoi polyhedra of the Th_3P_4 structure.

Acknowledgments

It is with pleasure that we acknowledge the valuable help of Miss Margaret O'Hara in the cardboard and scissors construction of the various Voronoi polyhedra as well as for other technical assistance. In addition we are happy to remember an interesting discussion of the Th_3P_4 structure with Professor E. W. Gorter in the summer of 1967. Further we would like to thank Dr. N. Tallan et al. for sharing with us advance information on their electrical and X-ray results for Eu_3S_4.

The computer programs used in the preparation of the figures include a contour drawing program by Branstetter (*45*), a plot program for the Gerber–Plotter by Blake (*46*), and two Algol programs by the author entitled "Interatomic Distances and Voronoi Polyhedra" and "Plotpolyhedra."

References

1. E. D. Eastman, L. Brewer, L. A. Bromley, P. W. Gilles, and N. L. Lofgren, *J. Amer. Chem. Soc.* **72**, 2248 (1950).
2. J. F. Miller, L. K. Matson, and R. C. Himes, *in* "Rare Earth Research" (J. F. Nachman and C. E. Lundin, eds.) p. 233, Gordon and Breach, New York (1961).
3. J. Flahaut, M. Guittard, M. Patrie, M. P. Pardo, S. M. Golabi, and L. Domange, *Acta Crystallogr.* **19**, 14 (1965).
4. M. Guittard, A. Benacerraf, and J. Flahaut, *Ann. Chim.* **9**, 25 (1964).
5. W. H. Zachariasen, *Acta Crystallogr.* **2**, 57 (1949).
6. E. Banks, K. F. Stripp, H. W. Newkirk, and R. Ward, *J. Amer. Chem. Soc.* **74**, 2450 (1952).
7. F. L. Carter, R. C. Miller, and F. M. Ryan, *Advanced Energy Conversion* **1**, 165 (1961).
8. S. W. Kurnick, R. L. Fitzpatrick, and M. F. Merriam, *in* "Rare Earth Research" (J. F. Nachman and C. E. Lundin, eds.), p. 249, Gordon and Breach, New York (1961).
9. M. Patrie, J. Flahaut, and L. Domange, *Rev. Hautes Temper. Et Refract.* **2**, 187 (1965).
10. V. Tien, J. Flahaut, and L. Domange, Compt. Rend. **262**, 278 (1966).
11. F. M. Ryan, I. N. Greenberg, F. L. Carter, and R. C. Miller, *J. Appl. Phys.* **33**, 864 (1962).
12. J. Appel, S. W. Kurnick, and P. H. Miller, Jr., "Metallurgy of Semiconductor Materials" (J. B. Schroeder, Ed.), p. 231, Interscience, New York (1961).
13. M. Cutler, J. F. Leavy, and R. L. Fitzpatrick, *Phys. Rev.* **133**, A1143 (1964).

14. M. CUTLER AND J. F. LEAVY, *Phys. Rev.* **133**, A1153 (1964).
15. O. BERKOOZ, M. MALAMUD, AND S. SHTRIKMAN, *Solid State Commun.* **6**, 185 (1968).
16. W. LUGSCHEIDER, H. PINK, K. WEBER, AND W. ZINN, *Z. Angew. Phys.* **30** (1), 36 (1970).
17. F. HOLTZBERG, P. E. SEIDEN, AND S. VON MOLNAR, *Phys. Rev.* **168**, 408 (1968).
18. S. W. KURNICK AND C. MEYER, *J. Phys. Chem. Solids* **25**, 115 (1964).
19. F. HOLTZBERG AND S. METHFESSEL, *J. Appl. Phys.* **37**, 1433 (1966).
20. F. HOLTZBERG, T. R. MCGUIRE, S. METHFESSEL, AND J. C. SUITS, *J. Appl. Phys.* **35**, 1033 (1964).
21. M. PATRIE, S. M. GOLABI, J. FLAHAUT, AND L. DOMANGE, Compt. Rend. **259**, 4039 (1964).
22. F. BERTAUT, *J. Phys. Radium* **13**, 499 (1952).
23. F. BERTAUT, "Ferroelectric and Dielectric Crystals: Contribution to the Theory of Fields, Potentials and Energies in Periodic Lattices," U.S. Air Force Report AD-22696, July, 1953.
24. M. BRUMEL AND F. DE BERGEVIN, *C.R. Acad. Sci. Paris*, **260**, 3598 (1965).
25. G. VORONOI, J. reine und angew. Math. **134**, 199 (1908).
26. J. D. BERNAL, *Nature (London)* **185**, 68 (1960).
27. F. W. SMITH, *Can. J. Phys.* **42**, 304 (1964).
28. E. W. GORTER, *J. Solid State Chem.* **1**, 279 (1970).
29. F. L. CARTER AND M. O'HARA, "Proceedings of the Eighth Rare Earth Research Conference" (T. A. Henrie, Ed.), p. 412, Reno, Nevada, Apr. 19–22 (1970).
30. F. L. CARTER, "Rare Earth Research III" (L. Eyring, Ed.), p. 495, Gordon and Breach, New York (1965).
31. F. HOLTZBERG, K. OKAYA, AND N. STEMPLE, *Abstr. Amer. Crystallogr. Ass. Meeting*, Gatlinburg, Tenn., p. 46 (1965).
32. W. L. COX, H. STEINFINK, AND W. F. BRADLEY, *Inorg. Chem.* **5**, 318 (1966).
33. A. V. VIRKAR, P. P. SINGH, AND A. RAMAN, *Inorg. Chem.* **9**, 353 (1970).
34. D. H. TEMPLETON, *J. Chem. Phys.* **23**, 1629 (1955).
35. R. E. JONES AND D. H. TEMPLETON, *J. Chem. Phys.* **25**, 1062 (1956).
36. K. SIEGBAHN, C. NORDLING, A. FAHLMAN, R. NORDBERG, K. HAMSIN, J. HEDMAN, G. JOHANSSON, T. BERGMARK, S. E. KARLSSON, I. LINDGREN, AND B. LINDBERG, "ESCA—Atomic, Molecular, and Solid State Structure Studied by Means of Electron Spectroscopy," 1st ed., North-Holland, Amsterdam-London (1967).
37. C. S. FADLEY, S. B. M. HAGSTROM, M. P. KLEIN, AND D. A. SHIRLEY, *J. Chem. Phys.* **48**, 3779 (1968).
38. D. H. TEMPLETON, *J. Chem. Phys.* **23**, 1826 (1955).
39. Q. C. JOHNSON AND D. H. TEMPLETON, *J. Chem. Phys.* **34**, 2004 (1961).
40. M. PICON AND J. FLAHAUT, *C.R. Acad. Sci. Paris* **243**, 2074 (1956).
41. B. H. DELONE, *Sov. Math.* **2** (3), 812 (1961).
42. F. L. CARTER, "Metallurgy of Semiconductor Materials" (J. B. Schroeder, Ed.), p. 245, Interscience, New York (1961).
43. I. BRANSKY, N. M. TALLAN, AND A. Z. HED, *J. Appl. Phys.* **41**, 1787 (1970).
44. H. H. DAVIS, I. BRANSKY, AND N. M. TALLAN, *J. Less-Common Met.* **22**, 193 (1970).
45. E. E. BRANSTETTER, "Contour, A Fortran Subroutine for Producing Contour Maps," Oak Ridge National Laboratory Report, ORNL-4031, Nov. 1966.
46. L. V. BLAKE, "Fortran Subroutines for Conversion of CalComp Plot Programs to Gerber-Plotter Paper-Tape Punching," Naval Research Laboratory, NRL Memorandum Report 2299, Aug. 1971.